Frascati Physics Series Vol. XXXVII (2004) pp. 367–374
Frontier Science 2004, Physics and Astrophysics in Space
Frascati, 14-19 June, 2004

CELESTE: DETECTING γ-RAYS ABOVE 30 GEV

Philippe Bruel [a]
for the CELESTE collaboration

[a] *Laboratoire Leprince-Ringuet, Ecole Polytechnique, 91128 Palaiseau, France*

Abstract

Since 2002, CELESTE has been running in an extended configuration. I report on the new results we have obtained on the Crab Nebula, Mrk421 and M31. I also present how we have improved our knowledge of the energy scale, and how we have reached a sensitivity of $\sim 6\sigma/\sqrt{\mathrm{h}}$ on the Crab.

1 Introduction

The CELESTE experiment [1] (as STACEE [2]) was designed in 1996 to detect γ-rays in the energy range between 30 and 300 GeV, not covered by satellites and Cherenkov imagers. In 1999, CELESTE used 40 heliostats and in 2000 we detected the Crab Nebula [3] with a threshold of 60 GeV and a sensitivity of $\sim 3\sigma/\sqrt{\mathrm{h}}$. Since 2000 we have improved several aspects of the experiment: we have increased the number of heliostats from 40 to 53 in 2002, we have reduced the systematic uncertainties and improved the sensitivity. Section 2 describes the CELESTE experiment. Section 3 is devoted to the knowledge of the energy scale. Section 4 describes the new data analysis, and the results on the Crab, Mrk421 and M31 are presented in section 5.

2 CELESTE

The CELESTE experiment uses 53 heliostats of a former solar plant at the THEMIS site (French Pyrénées) to detect γ-rays by sampling the Cherenkov light of their atmospheric showers. Each heliostat (54 m^2) reflects the light to the top of a tower, where the secondary optics and the photomultiplier tubes are located. The secondary optics allows the signals to be kept separate. Winston cones are placed at the entrance of each PMT such that the optical field of view of each heliostat is 10 mrad. This field of view is approximately the angular size of an electromagnetic shower in our energy range and helps to maximize the ratio of Cherenkov to night-sky light.

The heliostats are aimed at a single point, $P_{11\mathrm{km}}$, at 11 km above the ground and on the line passing through the center of the heliostat field in the direction of the observed source. In that configuration, the fields of view of the heliostats converge at the expected maximum point of Cherenkov emission for γ-ray showers in our energy range, allowing us to collect the largest number of photons.

The PMT signals are sent to the trigger electronics and the data acquisition system. The trigger system sums the individual analog signals by groups of 6 to 8 heliostats, and each sum enters a discriminator. A coincidence within 10 ns of at least 3 of the 6 groups is required to acquire the event. At each stage of the trigger, delays compensate for the changing optical path lengths. The trigger threshold is set above the night-sky light noise and is ~ 4.5 photoelectrons per heliostat. The trigger rate is ~ 25 Hz.

Each PMT signal is sent to a 1 GHz FADC (ETEP 301c). When a trigger occurs, a window of 100 samples (~ 100 ns) centered at the nominal Cherenkov pulse arrival time is read out. The photoelectron pulse width is ~ 4 ns.

The observations are made in the On-Off tracking mode: the observation of the source is followed or preceded by an observation at the same declination offset in right ascension by 20 minutes. The Off measurement is then used as a reference for the cosmic-ray background: the On-Off difference gives the source signal.

3 The knowledge of the energy scale

In order to reduce the uncertainty on the energy scale, we have improved our knowledge of the atmosphere and of the optical efficiency of CELESTE.

LIDAR

Since December 2001 a LIDAR [4] has been running at Themis. This LIDAR operates at two wavelengths: 532 nm (green) and 355 nm (UV). The data is used to extract the extinction profile up to ~ 15 km. The LIDAR allows us

to monitor the variations of the atmospheric opacity. So-called dust events (due to thick aerosol layers coming, for instance, from the Sahara) have been observed, in coincidence with other French network stations. During these dust events it has been possible to correlate the LIDAR measurements to the CELESTE trigger rate: the trigger rate clearly decreases as the atmospheric opacity increases, as expected. Apart from monitoring quick changes in the atmospheric conditions, LIDAR measurements have been used to derive a site-specific extinction parametrisation which we use in our simulation.

Photometry studies

The PMT anode currents are read out during observations and can be used to check the optical throughput and improve the quality of our simulation. The alignment of the heliostats are verified by mapping the images of bright stars: we measure these currents while spiraling around the star. Comparing these images to the ones obtained with the simulation showed us that we had to defocus the heliostats in the simulation. Furthermore, when a star is in the field of view of one heliostat, it is possible to compare the expected illumination to the one derived from the current measurement. This study showed us that we had a worse reflectivity than we thought. After these corrections, our simulation is in very good agreement with the observations.

4 Hadron rejection

Our first result on the Crab emission showed us that the discrimination between γ-ray induced showers and hadronic showers with CELESTE was not so easy. This was due to the narrow field of view of 10 mrad, which blurs the differences between electromagnetic and hadronic showers. We have tried to increase our sensitivity in two ways: a new pointing strategy and a new way of using the FADC data.

The veto pointing

In order to increase artificially the field of view, we have modified the pointing scheme: while 41 heliostats still aim the same point $P_{11\mathrm{km}}$, 12 other heliostats, called veto, aim 150 m aside, as seen in figure 1. Since γ-ray showers are more compact than hadron showers, no Cherenkov signal should be collected in the veto heliostats for a γ-ray shower. Thus, measuring a Cherenkov signal in a veto heliostat should be the signature of a hadronic shower. The figure 2 shows the distribution of N_{veto}, the number of veto heliostats with a significant Cherenkov signal, for simulated γ-rays and protons. We can see that $N_{veto} = 0$ for almost 100% of 50 GeV γ-rays, which is the case for only 30% of proton induced showers.

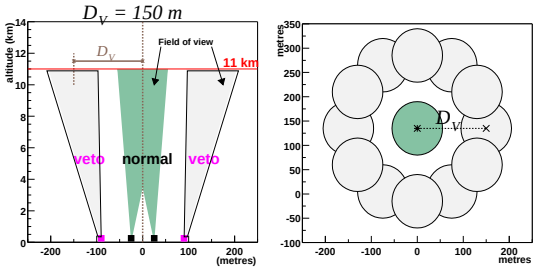

Figure 1: Principle of the veto pointing. Side view (left) and top view (right).

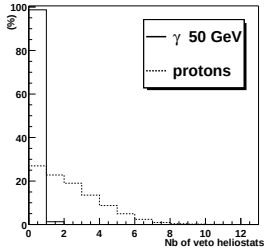

Figure 2: N_{veto} for simulated γ-rays and protons.

Summing the individual FADC information

For γ-rays between 30 and 300 GeV, the Cherenkov wavefront is spherical and its center $C_{11\mathrm{km}}$ can be assumed to lie somewhere in the plane $\mathcal{P}$ perpendicular to the source direction and passing through the point $P_{11\mathrm{km}}$. The analysis of the individual FADC channels can give the arrival time of the wavefront on each heliostat and it is thus possible to retrieve the position of $C_{11\mathrm{km}}$. In order to check the sphericity of the wavefront, one can use the individual arrival times, or use the width of the sum of the individual FADC channels.

But at very low energy, it is hardly possible to detect any significant Cherenkov signals in the individual channels. In that case, only the sum of the individual FADC windows exhibits a significant Cherenkov signal. We face a problem since summing the individual signals in the most coherent way requires compensating for the propagation delays, which implies knowing the position of $C_{11\mathrm{km}}$.

In order to overcome this difficulty we use the sum to find the position of $C_{11\mathrm{km}}$. For each point C of the plane $\mathcal{P}$, we apply the corresponding propagation delays (*i.e.* assuming that the wavefront is spherical and centered on C) before summing and measure the height H and the width W of the sum. For the right delay corrections, that is to say when $C = C_{11\mathrm{km}}$, the sum is the thinnest, or equivalently, the ratio H/W is the largest. The figure 3 shows the sum for one typical real event. The figure 4 shows how the ratio H/W varies in the plane $\mathcal{P}$ for one simulated 100 GeV gamma: this scan clearly exhibits a maximum which gives the position of $C_{11\mathrm{km}}$. This method allows the determination of the core position with a resolution of $\sim$ 15 m.

The figure 5 shows what we obtain for a single simulated 500 GeV proton: the distribution of H/W is not as sharp as for a gamma, as we expect, since the Cherenkov wavefront of a hadron shower is not spherical . We have estimated how sharp the H/W distribution is by evaluating how much smaller H/W

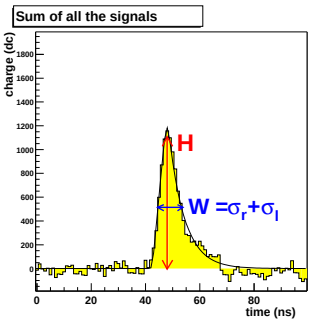

Figure 3: The sum of the individual FADC windows for a typical real event.

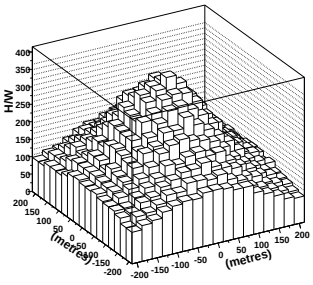

Figure 4: Scan of H/W over the plane $\mathcal{P}$ for one simulated gamma. The maximum gives the position of $C_{11\mathrm{km}}$.

is than its maximum value 200 m from $C_{11\mathrm{km}}$. The resulting variable ξ is shown in figure 6. For γ-rays, ξ takes low values (corresponding to sharp H/W distributions), for Off data it has larger values.

5 Results

The Crab Nebula

After selection cuts, we have 5 hours of data on the Crab. The data set is small because the weather conditions at Themis have been particularly bad since 2002. The figure 7 shows the ξ distribution for On and Off data, and the On-Off difference. This difference exhibits a clear excess which is reproduced by the γ-ray simulation. Imposing $\xi < 0.35$ gives a significance of 14 σ. Also shown is the On-Off difference of N_{veto} after the $\xi < 0.35$ cut: the excess is mainly due to events for which $N_{veto} = 0$, as expected for γ-rays. Requiring that $\xi < 0.35$ and $N_{veto} = 0$ gives a significance of 13 σ. The sensitivity of this analysis is $5.8\sigma/\sqrt{\mathrm{h}}$ and the signal/background ratio is $\sim 30\%$.

The figure 8 shows the energy distribution for a E^{-2} simulated spectrum at the transit of the Crab. We can see that the threshold after analysis cuts is still below 100 GeV, in spite of the optics degradation described in section 3.

Assuming that $E^2 \frac{dN}{dE} = kE^{\alpha+\beta \log_{10} E}$ and using the CAT spectrum [5] above 500 GeV, we have derived the integral flux of the Crab Nebula above 60 GeV: $I(E > 60\ \mathrm{GeV}) = 10.2^{+3.2}_{-3.1} \times 10^{-6}$ph m^{-2} s^{-1}. We have translated this measurement into a point in the $E^2 dN/dE$ plot. The figure 9 shows this new preliminary result, as well as our previous result and the results of EGRET and imagers.

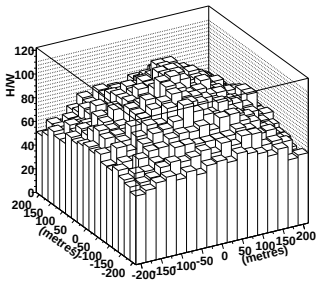

Figure 5: Scan of H/W over the plane $\mathcal{P}$ for one simulated proton.

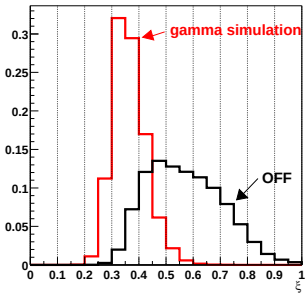

Figure 6: The ξ distribution for simulated gammas and Off data.

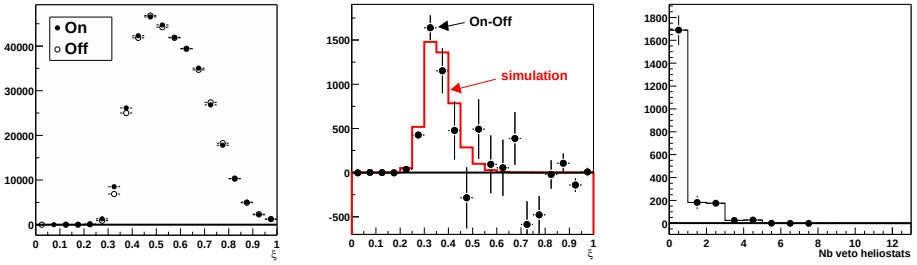

Figure 7: Crab data: On and Off distribution of ξ, On-Off distribution of ξ, On-Off distribution of N_{veto} for $\xi < .35$.

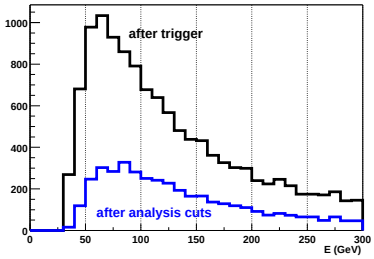

Figure 8: Energy distribution for a γ-ray E^{-2} simulated spectrum.

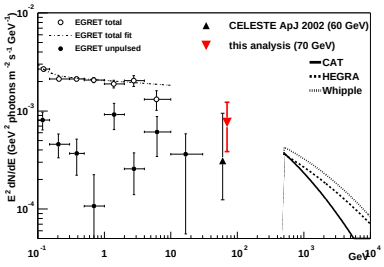

Figure 9: E^2dN/dE of the Crab.

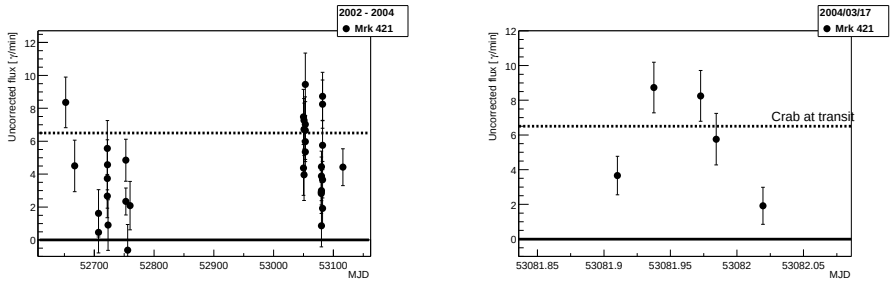

Figure 10: Light curve of Mrk421. Left: from January 2003 and April 2004. Right: one night (03/17/2004).

Markarian 421

After run selection, we have 10 hours of data on the blazar Markarian 421 between January 2003 and April 2004. After the cuts $\xi < 0.35$ and $N_{veto} = 0$, we have an excess of 19 σ. The figure 10 shows the uncorrected γ-ray rate for the entire observation period, and a zoom of a flaring night. It is interesting to note that the sensitivity reached by the new CELESTE analysis allows variability monitoring at the hour level.

Search for dark matter in M31

The possibility of γ-ray emission from M31 has been studied in [6], in the framework of neutralino annihilations. The rotation curve of M31 has been re-analysed with a more realistic mass-to-light ratio, leading to a spherical halo with a NFW profile. The supersymetric model predictions have been obtained with DarkSUSY and SUSPECT, in the minimal supergravity scenario (mSUGRA). In addition to standard phenomenological or theoretical constraints, we require the LSP relic density to verify $0.05 < \Omega_\chi h^2 < 0.2$.

After run selection, we have 10 hours of data. After analysis cuts, the On-Off difference is -0.9 σ, and we have derived an upper limit on the γ-ray flux above 50 GeV from M31. This upper limit is $\sim$ 3 orders of magnitude above the predicted fluxes.

6 Conclusions

CELESTE ended the week after this conference, but analyses are still in progress and new results should come next. They will take benefit of the recent improvements: a better knowledge of the energy scale, a better simulation, smaller systematic uncertainties, and a sensitivity of $\sim 6\sigma/\sqrt{\mathrm{h}}$ on the Crab.

For instance the new analysis will be applied to the data set obtained before 2002 (Crab, Mrk421 and Mrk501). CELESTE has already made spectrum measurements [7]. The energy resolution is $\sim$ 20% above 100 GeV. New spectrum measurements of the Crab and Mrk 421 will be obtained with the new data set.

References

[1] E. Paré *et al.*, NIM A490 (2002) 71-89

[2] J. Kildea, this conference

[3] M. de Naurois, J. Holder *et al.*, ApJ 566 (2002) 343-357

[4] J. Bussons Gordo *et al.*, in preparation

[5] C. Masterson *et al.*, Proc. Gamma 2001 Conf. (Baltimore) 590-594

[6] A. Falvard *et al.*, Astropart.Phys. 20 (2004) 467-484

[7] F. Piron *et al.*, Proc. 28th ICRC (Tsukuba 2001) 2607-2610